AGU PUBLICATIONS

JGR

Journal of Geophysical Research: Atmospheres

RESEARCH ARTICLE
10.1002/2013JD021159

Key Points:
- Ozone response to chlorine change depends on chlorine reservoir distributions
- Transport controls distributions of HCl and $ClONO_2$ in chemistry climate models
- Intermodel differences in ozone projections are explainable

Correspondence to:
A. R. Douglass,
Anne.R.Douglass@nasa.gov

Citation:
Douglass, A. R., S. E. Strahan, L. D. Oman, and R. S. Stolarski (2014), Understanding differences in chemistry climate model projections of stratospheric ozone, *J. Geophys. Res. Atmos.*, *119*, 4922–4939, doi:10.1002/2013JD021159.

Received 6 NOV 2013
Accepted 28 MAR 2014
Accepted article online 1 APR 2014
Published online 24 APR 2014

Understanding differences in chemistry climate model projections of stratospheric ozone

A. R. Douglass[1], S. E. Strahan[2], L. D. Oman[1], and R. S. Stolarski[3]

[1]NASA Goddard Space Flight Center, Greenbelt, Maryland, USA, [2]Universities Space Research Association, Columbia, Maryland, USA, [3]Department of Earth and Planetary Sciences, Johns Hopkins University, Baltimore, Maryland, USA

Abstract Chemistry climate models (CCMs) are used to project future evolution of stratospheric ozone as concentrations of ozone-depleting substances (ODSs) decrease and greenhouse gases increase, cooling the stratosphere. CCM projections exhibit not only many common features but also a broad range of values for quantities such as year of ozone return to 1980 and global ozone level at the end of the 21st century. Multiple linear regression is applied to each of 14 CCMs to separate ozone response to ODS concentration change from that due to climate change. We show that the sensitivity of lower stratospheric ozone to chlorine change $\Delta O_3/\Delta Cl_y$ is a near-linear function of partitioning of total inorganic chlorine (Cl_y) into its reservoirs; both Cl_y and its partitioning are largely controlled by lower stratospheric transport. CCMs with best performance on transport diagnostics agree with observations for chlorine reservoirs and produce similar ozone responses to chlorine change. After 2035, differences in $\Delta O_3/\Delta Cl_y$ contribute little to the spread in CCM projections as the anthropogenic contribution to Cl_y becomes unimportant. Differences among upper stratospheric ozone increases due to temperature decreases are explained by differences in ozone sensitivity to temperature change $\Delta O_3/\Delta T$ due to different contributions from various ozone loss processes, each with its own temperature dependence. Ozone decrease in the tropical lower stratosphere caused by a projected speedup in the Brewer-Dobson circulation may or may not be balanced by ozone increases in the middle- and high-latitude lower stratosphere and upper troposphere. This balance, or lack thereof, contributes most to the spread in late 21st century projections.

1. Introduction

If anthropogenic ozone-depleting substances (ODSs) were the only change in atmospheric composition, ozone (O_3) and stratospheric chlorine would be expected to return to unperturbed levels as ODSs were removed from the atmosphere. Other concurrent changes in composition complicate the picture, and the anticipated increases in greenhouse gas (GHG) concentrations leading to stratospheric cooling and circulation changes are also expected to impact the future global ozone distribution. Stratospheric cooling causes ozone to increase by slowing temperature-dependent ozone loss processes [e.g., *Haigh and Pyle*, 1982]. All chemistry climate models (CCMs) predict a speedup in the Brewer-Dobson circulation, leading to a decrease in stratospheric tropical ozone column and increased ozone in middle and high latitudes, depending on the structure of the circulation change [*Austin and Wilson*, 2006; *Shepherd*, 2008; *Waugh et al.*, 2009; *Butchart et al.*, 2010]. In spite of commonalities in ozone evolution that is simulated by the suite of CCMs as noted by *Oman et al.* [2010], there are significant differences in the projections and they are the subject of this work.

Eyring et al. [2005] describe the ongoing community effort, sponsored by World Climate Research Programme project Stratosphere-troposphere Processes and their Role in Climate (SPARC), to evaluate CCMs (Chemistry-Climate Model Validation Activity (CCMVal)). The CCMVal project used diagnostics developed from observations to evaluate dynamical, chemical, and radiative processes in CCMs. The CCMs, their simulations, and the results of the evaluations are described in the CCMVal report [*Stratosphere-troposphere Processes and their Role in Climate Chemistry-Climate Model Validation Activity* (*SPARC CCMVal*), 2010, hereinafter CCMVal2010]. These simulations were also contributed to the World Meteorological Organization *Scientific Assessment of Ozone Depletion*: *2010* [*WMO* (*World Meteorological Organization*), 2011, hereinafter WMO2011]. Although CCMVal used observations to show that chemical and transport processes were not well represented by the CCMs in all cases, this information was not used to discriminate among CCMs. Projections of 21st century ozone used in WMO2011 were obtained using a time series additive model (TSAM) method to produce multimodel trends (MMTs). The TSAM method as adopted in Chapter 9 of

©2014. American Geophysical Union. All Rights Reserved.

CCMVal2010 and *Scinocca et al*. [2010] has three steps: estimation of trends from individual CCMs, baseline adjustment, and combination of the individual trends to produce the MMT. The formalism permits the use of weights based on performance metrics or other criteria when combining the individual trends, but this feature was not used. An important aspect of this method is that the residuals of the trend estimate satisfy assumed properties of noise. The CCMs participating in CCMVal and WMO2011 are not completely independent as they share common elements such as the advection scheme or core general circulation model. Perhaps more important, the CCMVal2010 evaluation reveals deficiencies for some CCMs such as nonconservation of mass, missing chemical reactions, or poor representation of various processes that result in poor comparisons of constituent distributions with observations. Here we consider the differences among CCM projections in detail with the goal of identifying aspects of these differences that are explained by deficiencies, seeking to discern whether aspects of performance explain the differences or whether they are appropriately considered "noise."

Waugh and Eyring [2008] compare projections for total column ozone (TCO) obtained using performance metrics to weight the contributions from various CCMs with an unweighted multimodel mean and found only small differences between these weighted and unweighted projections. Their analysis also revealed some issues with the strategy of weighting contributions to obtain a better projection, noting that the diagnostics were not independent of each other. In addition, performance on a particular diagnostic of the present atmosphere might or might not be related to the ozone response to composition change.

Recent studies have taken a different approach to the use of diagnostics of chemistry and transport to explain differences among simulations. *Strahan et al*. [2011] built on the transport diagnostics for the lower stratosphere from Chapter 5 of CCMVal2010 using comparisons with nitrous oxide and mean age to reveal details of tropical ascent and isolation. *Strahan et al*. [2011] show that the four CCMs with the most realistic representation of transport, and no significant errors or omission in their chemical mechanism or its implementation (Chapter 6 of CCMVal2010), produce a much narrower range of predicted TCO return-to-1980 dates for the 60°S–60°N total column ozone than the suite of CCMs that contributed simulations to CCMVal2010 and WMO2011. *Douglass et al*. [2012] examined the upper stratospheric ozone response to changes in ODS level and cooling due to increased levels of GHGs. Upper stratospheric ozone is controlled by the reaction $O + O_3 \rightarrow 2\ O_2$ and catalytic loss cycles involving chlorine, nitrogen, and hydrogen radicals that have the same net effect. The temperature dependence of the loss processes varies; $O + O_3$ is most temperature dependent, and the chlorine catalytic cycle is least. *Douglass et al*. [2012] showed that the CCMs produce a wide, often unrealistic, range of upper stratospheric temperatures for the present atmosphere. Together that range and differences in levels of constituents such as reactive nitrogen account for differences in the relative importance of the catalytic loss cycles in the upper stratosphere. All of the CCMs predict increases in upper stratospheric ozone as anthropogenic chlorine and temperatures decrease in the 21st century, and their projected temperature decreases are similar. However, there are differences in the projected ozone increases that become larger as anthropogenic chlorine decreases because the ozone sensitivity to temperature change varies among CCMs. No analysis to date elucidates the link between transport and lower stratospheric chemistry implied by the *Strahan et al*. [2011] result.

This paper demonstrates that many of the differences in the predicted evolution of stratospheric ozone can be interpreted and understood using a subset of CCMVal diagnostics and concepts that describe interactions among photochemical, transport, and radiative processes that control stratospheric ozone. We apply multiple linear regression (MLR) to the future simulations used in the CCMVal exercise and WMO2011 in order to separate contributions of ODS change from other factors that contribute to future ozone evolution. MLR has been successfully applied to observational data sets and CCM output to quantify the ozone response to ODS change by accounting for other factors known to affect ozone levels such as volcanic injection of stratospheric aerosols, solar cycle variability, and the quasi-biennial oscillation [e.g., *Stolarski et al*., 1991, 2006]. This approach was also applied to future simulations to separate the temperature and ozone response to ODS change from that due to other changes in composition and climate [*Stolarski et al*., 2010; *Oman et al*., 2010]. The results of this separation will then be examined with two goals. The first is to explain the narrower range of values for the predicted year of total column ozone return to 1980 that is obtained from CCMs with the most realistic performance on transport diagnostics as detailed by *Strahan et al*. [2011]. This part of the analysis focuses on the simulated ozone responses to changes in ODSs, in particular anthropogenic

©2014. American Geophysical Union. All Rights Reserved.

Table 1. Models That Contributed a Future Scenario Simulation, Identifying CCMs With Most Realistic Transport as Discussed by *Strahan et al.* [2011]

Model No.	Model Name	Reference	Most Realistic Transport [*Strahan et al.*, 2011]
1	AMTRAC3	*Austin and Wilson* [2010]	
2	CCSRNIES	*Akiyoshi et al.* [2009]	
3	CMAM	*Scinocca et al.* [2008]; *de Grandpré et al.* [2000]	realistic transport
4	CNRM-ACM	*Déqué* [2007]; *Teyssèdre et al.* [2007]	
5	GEOSCCM	*Pawson et al.* [2008]	realistic transport
6	LMDZrepro	*Jourdain et al.* [2008]	
7	MRI	*Shibata and Deushi* [2008a, 2008b]	
8	Niwa-SOCOL	*Schraner et al.* [2008]	
9	SOCOL	*Schraner et al.* [2008]	
10	ULAQ	*Pitari et al.* [2002]	
11	UMSLIMCAT	*Tian and Chipperfield* [2005]; *Tian et al.* [2006]	realistic transport
12	UMUKCA-METO	*Davies et al.* [2005]; *Morgenstern et al.* [2009]	
13	WACCM	*Garcia et al.* [2007]	realistic transport
14	UMUKCA-UCAM	*Davies et al.* [2005]; *Morgenstern et al.* [2009]	

chlorine. The second goal is to explain the differences in the ozone response to the ongoing changes in GHGs (excluding ODSs) that lead to changes in stratospheric circulation and temperature. These differences in response cause the future simulations to diverge from one another in the middle to late 21st century.

The simulations and the CCMs that produce them are briefly described in section 2. Section 2 also describes data sets that contribute to interpretation of the simulated ozone evolution. The analysis strategy and results are presented in section 3. Section 4 describes relationships between the sensitivity of simulated ozone to chlorine change and the simulation of the present atmosphere. Section 5 considers ozone after 2035 as the anthropogenic contribution to chlorine levels decreases and the ozone response to climate change becomes dominant. Results and their implications are summarized in section 6.

2. Chemistry Climate Models, Simulations, and Data

2.1. CCMVal Models and Simulations

Morgenstern et al. [2010] and *Oman et al.* [2010] present a detailed overview of the models, inputs, and scenarios used in the CCMVal-2 exercise. These models contributed simulations that were evaluated in CCMVal2010 and used in WMO2011 Chapter 2 (Stratospheric Ozone and Surface Ultraviolet Radiation) [*Douglass and Fioletov et al.*, 2011] and Chapter 3 (Future Ozone and Its Impact on Surface UV) [*Bekki and Bodeker et al.*, 2011]. Eighteen groups contributed simulations to CCMVal-2, but for this analysis we include only the 14 models that contributed a future scenario simulation and whose vertical domain includes the upper stratosphere. These models are listed in Table 1, where CCMs with most realistic transport as discussed by *Strahan et al.* [2011] are identified. The future scenario (referred to as REF-B2) uses the A1B greenhouse gas (GHG) scenario from the *IPCC* (*Intergovernmental Panel on Climate Change*) [2000] and the revised A1 halogen scenario from *WMO* (*World Meteorological Organization*) [2007] and CCMVal2010. Most models have simulations that cover 1960–2099 with 10 year model spin-up prior to 1960. The Unified Model/United Kingdom Chemistry Aerosol Community Model–Met Office (UMUKCA-METO) future simulation ends in 2083.

2.2. Observations

We use observations to show how the simulated distributions of reservoir gases hydrogen chloride (HCl) and chlorine nitrate ($ClONO_2$) depend on realistic lower stratospheric transport in order to establish context for discussion. We otherwise do not repeat the comprehensive evaluation of photochemistry in Chapter 6 of CCMVal2010.

2.2.1. Network for the Detection of Atmospheric Composition Change

A primary goal of the Network for the Detection of Atmospheric Composition Change (NDACC) is to obtain consistent, standardized, long-term measurements of atmospheric trace gases at a set of globally distributed research stations to detect trends in atmospheric composition. Here we consider time series of the total column abundances of HCl and $ClONO_2$ obtained using Fourier transform infrared spectrometers (FTIRs) from

©2014. American Geophysical Union. All Rights Reserved.

Table 2. NDACC Stations and Their Locations

Station	Location
Kiruna, Sweden	67.84°N 20.41°E
Harestua, Norway	60.2°N 10.8°E
Jungfraujoch, Switzerland	46.55°N 7.98°E
Kitt Peak, AZ, USA	31.9°N 111.6°W
Izaña (Tenerife), Spain	28.30°N 16.48°W
Mauna Loa, HI, USA	19.54°N 155.58°W
Lauder, New Zealand	45.04°S 169.68°E

eight of the long-term measurement sites listed in Table 2. These sites were selected from the 18 FTIR locations listed in the measurements and analysis subdirectory to encompass a broad latitude range with temporal records of 9 years or longer. *Rinsland et al*. [2003] discuss such measurements in detail and show that the buildup and leveling off of the sum of HCl and $ClONO_2$ columns from six of these sites and others not included here are consistent with time series for surface source gases and with upper stratospheric HCl as measured by the Halogen Occultation Instrument on the Upper Atmosphere Research Satellite, confirming the effectiveness of the Montreal Protocol and its amendments and adjustments in reducing the anthropogenic contribution to atmospheric chlorine. A recent study by *Kohlhepp et al*. [2012] shows a decrease of chlorine-containing species of ~1%/yr between 2000 and 2009. Details about the measurements are provided by *Rinsland et al*. [2003, and references therein] and can also be obtained from the NDAAC website http://www.ndacc.org/.

2.2.2. SCISAT Atmospheric Chemistry Experiment

The Atmospheric Chemistry Experiment (ACE) on the Canadian satellite SCISAT-1 is a Fourier transform spectrometer (FTS). ACE-FTS is a solar occultation instrument that obtains high-resolution spectra (0.02 cm^{-1}) between 750 and 4400 cm^{-1} [*Bernath et al*., 2005]. ACE-FTS makes daily measurements in each of two latitudes bands for sunrise and sunset. Vertical profiles are retrieved for up to 15 sunrises and 15 sunsets per day. *Mahieu et al*. [2005] discuss validation of Version 1 retrievals for $ClONO_2$ and HCl profiles obtained from ACE-FTS. Here we use Version 3 $ClONO_2$ and HCl profiles, focusing on middle latitudes between 50 hPa and 10 hPa.

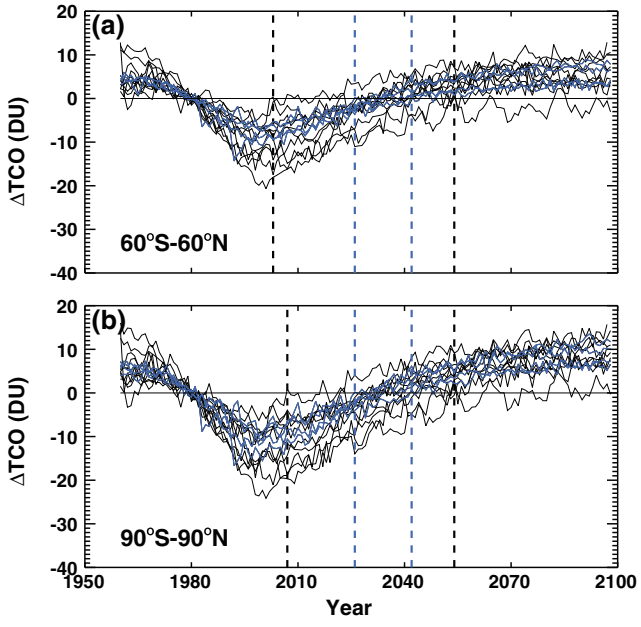

Figure 1. (a) The evolution of 60°S–60°N TCO, referenced to the 1978–1982 mean, as simulated by CCMVal models. (b) Same as Figure 1a for 90°S–90°N. In Figures 1a and 1b the blue traces identify CCMs with most realistic transport. The dashed black vertical lines indicate the range of years for return to 1980 for the entire group of CCMs; the blue vertical lines indicate the narrower range for the CCMs with most realistic transport.

3. MLR Analyses of CCM Ozone Columns

3.1. Total Column Ozone Time Series in CCMs

Figure 1 shows the evolution of 60°S–60°N and 90°S–90°N averages of total column ozone (TCO) simulated by the CCMVal models, referenced to 1980. The 1980 mean is approximated by a 5 year average of annual means (1978–1982) to reduce the importance of year-to-year variations. The range of differences among simulations in 2100 (~10 Dobson unit (DU)) is substantially smaller than the range in 2000 (~15 DU) when the stratospheric chlorine was near its peak value. However, the simulated range of ozone change between 1980 and 2000 is unrealistically large compared with the estimates of ozone depletion obtained from observations. WMO2010 reported 60°S–60°N column ozone levels for 2000–2010 to be 3.5% (~10 DU) less than 1980, comparable to the range of simulated increases in global column ozone in 2100 relative to 1980.

©2014. American Geophysical Union. All Rights Reserved.

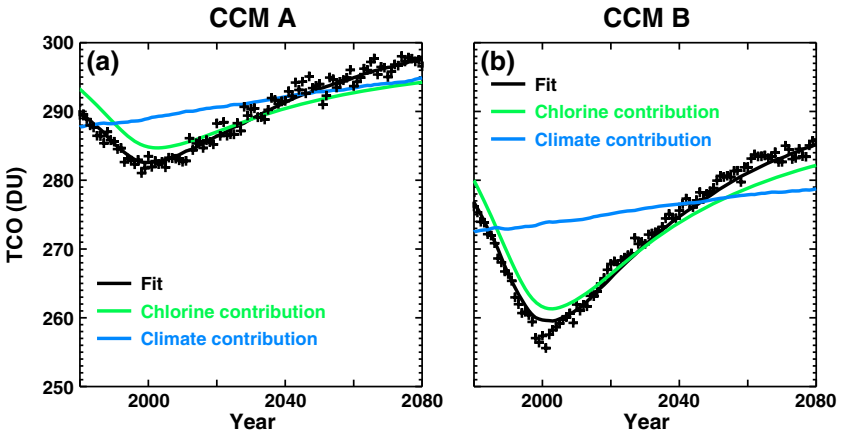

Figure 2. (a) 60°S–60°N TCO from one of the CCMs. The crosses are the annually averaged columns; the black, green, and blue lines are the fit obtained using the MLR, the contribution due to chlorine change, and the contribution due to climate change, respectively. (b) Same as Figure 2a for a second CCM. The contributions to ozone change from climate change are similar in these examples, but contributions from chlorine change differ by more than a factor of 2.

In each panel of Figure 1 the four blue traces identify the simulations from the CCMs that have the most realistic transport based on comparisons with N_2O and mean age presented by *Strahan et al.* [2011]. The black dashed vertical lines indicate the earliest and latest years for return to 1980; the blue dashed vertical lines show the narrower range of return years for the CCMs with realistic transport. These ranges are nearly the same for the 60°S–60°N and 90°S–90°N averages. The differences from the 1980 mean are more negative around 2000 and more positive beginning ~2050 for the global average compared with the 60°S–60°N average. The contribution from springtime lower stratosphere polar ozone loss that is included in the global average explains the more negative difference in 2000. Acceleration of the Brewer-Dobson circulation, predicted by all CCMs [*Butchart et al.*, 2006, 2010], causes a tropical ozone decrease that is countered by middle- and high-latitude ozone increases [*Li et al.*, 2009]. The 90°S–90°N average includes more of the lower stratosphere middle- and high-latitude ozone increases than the 60°S–60°N average, explaining the more positive differences from 1980 after 2050 for the 90°S–90°N averages compared with the 60°S–60°N averages. Because the differences among the simulations are similar for the both spatial averages, further discussion considers only the 60°S–60°N that was discussed by *Strahan et al.* [2011] and is commonly considered in the WMO assessments.

Figure 1 suggests important differences in CCM responses to changes in ODS concentrations between 1980 and 2000 in spite of using identical source gas boundary conditions. In order to quantify and explain such differences in the ozone sensitivity to changes in composition and climate, our strategy is to analyze the output from each CCM using multiple linear regression (MLR). This method, which has been applied to observed and simulated time series [*Stolarski et al.*, 1991, 2010], capitalizes on the length of the simulated time series to separate the contributions of ODS change (also referred to as chlorine change) and climate change (i.e., circulation and temperature) to ozone evolution. For each CCM the time series used in the MLR begins in 1960 and extends to 2083 for the shortest simulation and to within 1 or 2 years of 2100 for the others.

The same time series of equivalent effective stratospheric chlorine (EESC) [*Newman et al.*, 2007] is used to represent ODS change in the MLR analysis of all CCMs. We explored several options for explanatory variables for circulation or climate-related changes. Most of the CCMs provided time series of monthly averages for the 20°S–20°N transformed Eulerian mean vertical velocity (w^*) at 70 hPa. In order to identify an explanatory variable useful for all of the CCMs, we tested the normalized time series of lower tropical stratosphere vertical gradients in the long-lived tracer nitrous oxide (N_2O) and also tested a simple linear trend. All options produce similar values for the ozone sensitivities to EESC (chlorine) change within each CCM. Results for ozone sensitivity to climate change (including both changes in temperature and circulation) are equivalent using either w^* or the N_2O gradients, suggesting that use of N_2O gradients is acceptable for the CCMs that did not provide information for w^*. For most CCMs, the time dependence of w^* or the N_2O is nearly linear, and the same results are obtained using a linear trend. Results for two CCMs with a linear response to climate change are shown in Figure 2. In each panel, the crosses are the annual average ozone between 60°S and 60°

©2014. American Geophysical Union. All Rights Reserved.

N from a particular CCM. The black solid line is the fit to the simulation obtained from MLR. The green line is the mean value plus the contribution to the temporal evolution due to chlorine change; the blue line is the mean value plus the contribution due to changes in climate. The fits obtained from the MLR capture the time dependence of each simulation. In these examples, the sensitivity to climate change is similar, but the sensitivity to chlorine change differs markedly. Other CCMs have similar sensitivity to chlorine change but differing sensitivity to climate change (not shown). MLR fitting facilitates comparisons among CCMs by reducing noise due to interannual variability when computing ozone differences for various time periods.

In all of the CCMs, most of the change in TCO from 1980 to 2000 is due to chlorine change. For the ensemble of simulations, the mean and standard deviation of the ozone decrease between 1980 and 2000 attributed to chlorine increase are −9.4 DU and 4.0 DU.

The mean and standard deviation of the ensemble of ozone change due to climate change are 0.8 DU and 0.7 DU, respectively. For the examples in Figure 2, the 60°S–60°N ozone change between 1980 and 2000 due to climate changes is ~1.25 DU. In contrast, the 60°S–60°N ozone changes due to chlorine increase are −8.4 DU and −18.4 DU.

3.2. Ozone Response in the Upper and Lower Stratosphere

Projected changes in GHGs and ODSs will have different impacts on the upper and lower stratospheric ozone. The ozone response to these composition changes is a function of altitude because the time scales of processes controlling ozone vary with height. In the upper stratosphere, fast radical photochemistry controls the ozone level on time scales of days, while transport controls O_3 on seasonal to multidecadal time scales through the slowly changing levels of long-lived source gases and reservoir species that control the levels of total reactive nitrogen (NO_y) and Cl_y. In the lower stratosphere where ozone is long lived, the chemical and transport processes both contribute to the ozone evolution. The predicted speedup in the Brewer-Dobson circulation will affect processes controlling ozone at all time scales through its effects on composition, chemistry, transport, and temperature.

In addition to its application to the total column ozone as discussed in the previous section, here we use MLR to quantify the effects of GHG and ODS changes on ozone in two partial columns: from the upper troposphere through the midstratosphere (500 hPa–20 hPa) and the upper stratosphere (20 hPa–1 hPa). As for the TCO, MLR is applied to time series from 1980 to the final simulated year for each CCM. Ideally, the partial column for the upper troposphere through the midstratosphere would be computed from a level at or near each CCM tropopause to 20 hPa. The archived fields from the CCMs have only 31 levels from 1000 hPa to 0.1 hPa, with no specific information on tropopause location. We computed partial columns with the lower boundary at 500 hPa, 400 hPa, 300 hPa, and 200 hPa, with the exception of SLIMCAT that has a lower boundary at 170 hPa. The changes from 1980 that are discussed here are insensitive to the lower boundary for most CCMs; ozone profiles from two CCMs suggest a lower tropopause. We present results using 500 hPa as the lower boundary for this partial column to include middle- and high-latitude upper troposphere ozone increases due to circulation changes that contribute to the change in TCO. Of the models listed in Table 1, only ULAQ includes a comprehensive representation of tropospheric chemistry (Chapter 2 of CCMVal2010), and the tropospheric contribution to the total column ozone change is small.

Ozone changes from 1980 are computed from the resulting MLR fits for 2000, a period during which chlorine loading increased rapidly and for 2035, near the midpoint of the range of return years (2026–2040) for the CCMs with realistic transport identified by *Strahan et al*. [2011]. The TCO differences and the contributions from each of the two partial columns are shown for each CCM in Figure 3. Here and in following figures of similar style the CCM number on the *x* axis matches the CCM number in Table 1. Note that in 2035 the ozone changes referenced to 1980 that are due to ODS change and climate change make similar contributions to the differences in projections as will be discussed in the following section.

Figure 3a shows that while chlorine loading is increasing (1980–2000), ozone changes are negative in both the lower and upper columns in most CCMs. The TCO changes among the CCMs range from −3 to −17 DU; most of this variance comes from the differences in the lower column. For the ozone change between 2035 and 1980 (Figure 3b), lower column changes are negative in most CCMs, whereas the upper column changes are positive or less than −0.7 DU. The TCO change can be positive (beyond "recovery"), near zero (recovery), or

©2014. American Geophysical Union. All Rights Reserved.

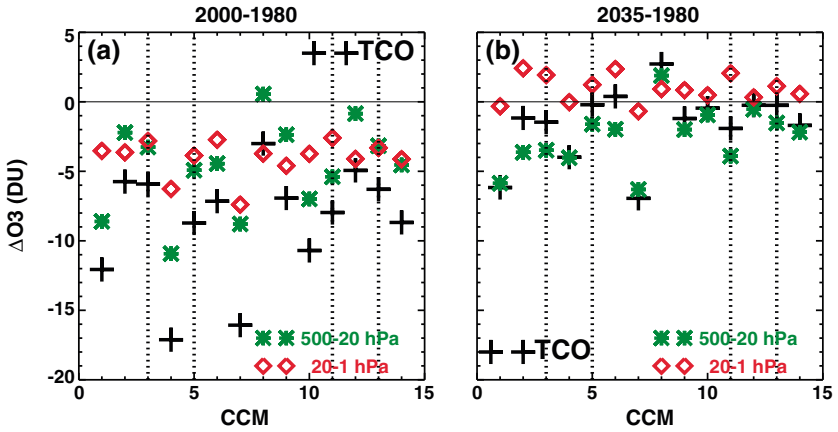

Figure 3. (a) The changes in 60°S–60°N TCO between 1980 and 2000 (black pluses), the contribution from 20 hPa–1 hPa (red diamonds), and the contribution from 500 hPa–20 hPa (green stars). (b) Same as Figure 3a for the changes between 1980 and 2035. For both time intervals, the lower region contributes more to the differences in CCM projections than upper region. The dotted vertical lines identify the CCMs with most realistic transport.

negative (not yet recovered). The range of predicted TCO difference for 2035–1980 (standard deviation 2.6 DU) is less than that predicted for 2000–1980 (standard deviation 4.1 DU). The lower column changes in this period again contribute the most to the differences among projections.

3.3. Contributions of Chlorine and Climate Change to Ozone Response

3.3.1. Total Column Ozone Changes

In Figure 4 we separate the chlorine and climate change contributions to the TCO change to explain the variance among CCMs shown in Figure 3b. Ten CCMs, including the four with the most realistic transport, are clustered near the vertical dashed line, showing the balance between the contributions of chlorine change and climate change among these CCMs that are close to 1980 O_3 levels by 2035. Among these CCMs, the TCO change between 1980 and 2035 is most negative for those with the smallest increase due to climate change. Three of the CCMs that are 4 DU or more from their 1980 values are among those with the greatest change due to chlorine; two of these three have negative ozone response due to climate change. The CCM with the earliest recovery (more than 2.5 DU greater than 1980 in 2035) has weak sensitivity to chlorine change and the most positive response to climate change.

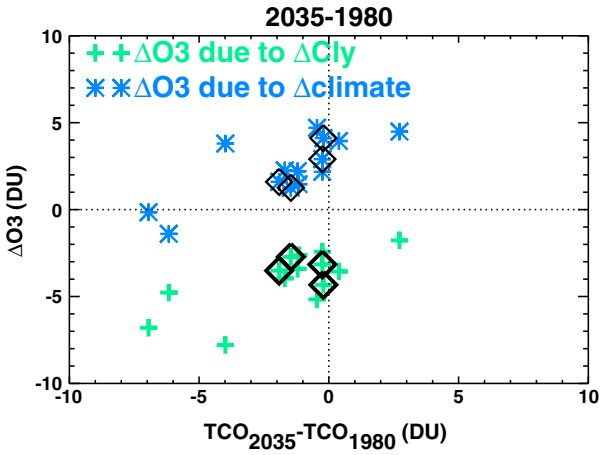

Figure 4. The 2035–1980 60°S–60°N contribution due to chlorine change (green pluses, *y* axis) and that due to climate change (blue stars, *y* axis) as functions of the change in TCO (*x* axis). The black diamonds indicate the CCMs with most realistic transport.

3.3.2. Separation of Processes Affecting Lower and Upper Ozone Columns

From 1980 to 2000, the correlation between the lower and upper column ozone responses is 0.6; chlorine-related processes (but not the same processes) dominate the loss in both regions. The correlation gradually declines to 0.2 between 2000 and 2050, as ODS levels decrease and the contributions from climate change increase. This change in correlation suggests that different mechanisms control the ozone response during different time periods and that the lower and upper column ozone responses to climate change are not correlated. This prompts separate investigation of the processes contributing to lower and upper column ozone changes from 1980.

Douglass et al. [2012] show that upper stratospheric ozone levels prior to 1980 are

©2014. American Geophysical Union. All Rights Reserved.

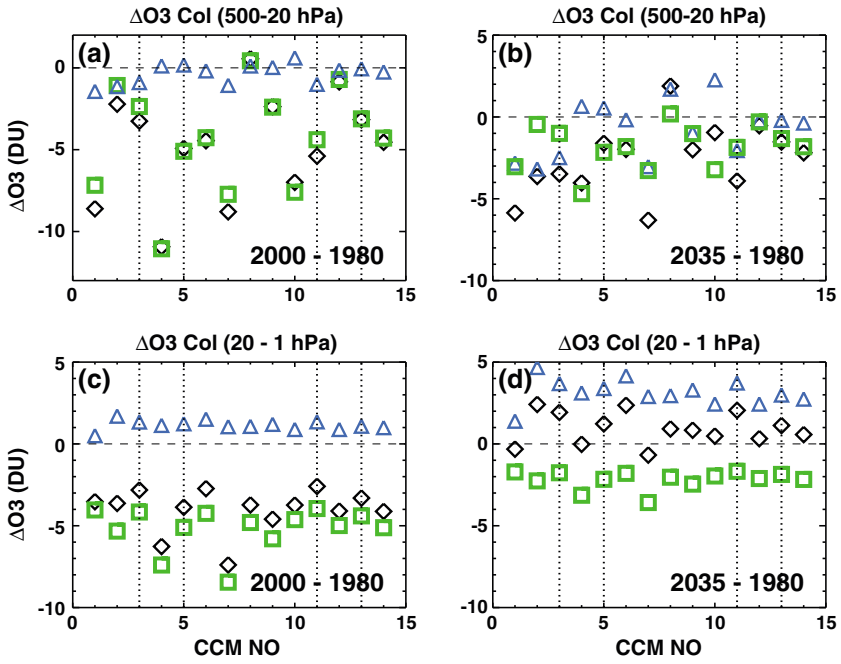

Figure 5. (a) The change in 60°S–60°N partial ozone column (500 hPa–20 hPa) between 2000 and 1980 (black diamonds), the contribution due to chlorine change (green squares), and the contribution due to climate change (blue triangles). (b) Same as Figure 5a for 2035 and 1980. (c) Same as Figure 5a for the partial ozone column (20 hPa–1 hPa). (d) Same as Figure 5c for the 2035 and 1980. The dotted vertical lines identify the CCMs with most realistic transport.

higher for the CCMs with colder temperatures in the upper stratosphere and vice versa. They use the framework developed by *Stolarski and Douglass* [1985] to explain how differences in unperturbed values for ozone level, temperature, and reactive nitrogen contribute to differences in sensitivity of ozone to perturbations in temperature and chlorine. The amplitude of the temperature-dependent annual cycle in ozone varies as expected, decreasing as chlorine increases in all CCMs because the chlorine-catalyzed loss cycle is less dependent on temperature than other ozone loss cycles. In the lower stratosphere both photochemical and transport terms are important. In this section, we apply the MLR to time series of the upper and lower partial columns in order to separate the ozone change related to chlorine from other processes. We present results for two time periods.

Figure 5a shows the simulated ozone changes in the lower column from 1980 to 2000. The response due to chlorine increase (green diamonds) greatly exceeds the ozone change due to climate change (blue triangles) in all but one of the CCMs. In addition, ozone response to increased chlorine contributes much more to intermodel differences than the response to climate change (4.3 DU and 0.6 DU standard deviations, respectively). In comparison, the lower column difference between 1980 and 2035 due to chlorine is less than half the difference between 1980 and 2000, and there is also less variance among CCMs (Figure 5b). Although still elevated substantially compared with 1980 (50–100% larger), by 2035, middle-latitude lower stratospheric inorganic chlorine has decreased by 20–40% from its peak value, depending on the pressure level and CCM being examined, explaining the smaller contribution from chlorine related processes. The differences among the climate change responses between 2035 and 1980 are larger than those for chlorine.

Changes in the 20 hPa–1 hPa ozone partial columns between 1980 and 2000 (Figure 5c) are broadly similar to the changes computed for the 500 hPa–20 hPa ozone partial columns but exhibit significantly less model-to-model variability (Figure 5a). The ozone changes due to chlorine increase dominate the overall response in all CCMs and account for the differences among projections. The ozone response to climate change is positive and about 1.1 DU in all CCMs. By 2035 (Figure 5d), the ozone change due to chlorine change has decreased, while the O_3 increase due to climate change has increased; this increase is both larger and more variable than the ozone decrease due to chlorine. *Douglass et al.* [2012] show that temperature changes are comparable among CCMs; thus, the differences in ozone response to climate change reflect differences in

©2014. American Geophysical Union. All Rights Reserved.

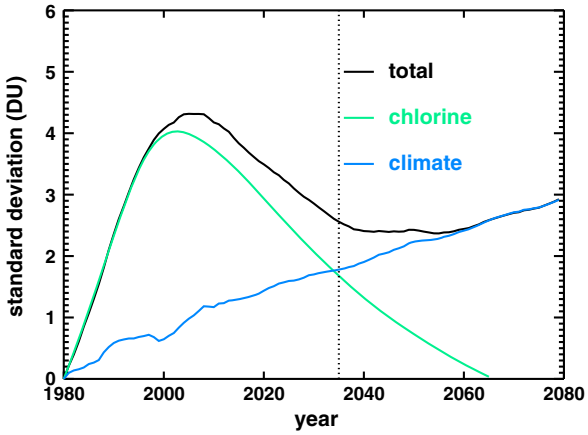

Figure 6. The standard deviation of CCM TCO differences from 1980 for each year between 1980 and 2080. The MLR results are used to produce separate time series for the contribution due to chlorine change and the contribution due to climate change. The standard deviations are shown here for the difference in TCO (black), the chlorine contribution (green), and the contribution due to climate change (blue).

ozone sensitivity to temperature. Ozone sensitivity to climate change is similar among CCMs in 2000 and different in 2035. This is expected because when ozone loss due to chlorine is a larger fraction of all losses, as in 2000, O_3 is less sensitive to temperature change because the chlorine loss reaction is the least temperature dependent of all the loss processes.

Figure 6 shows how the standard deviation among the 14 simulations of the 60°S–60°N TCO differences from 1980 changes between 1980 and 2080, separating the contributions from chlorine change (green) and climate change (blue). Until about 2000, the differences in ozone sensitivity to chlorine change account for nearly all of the variation among CCM projections. The contribution from climate change rises throughout the integration, equaling the contribution from chlorine change in about 2035. The chlorine contribution to intermodel differences continues to decline as expected as chlorine declines, while the contribution of climate change continues to increase. By 2080, the differences in chlorine sensitivity do not contribute significantly to intermodel differences, and the climate change contribution is ~70% of the magnitude of the peak chlorine contribution in 2005.

4. Explaining Differences in Ozone Projections

Figure 1 shows that in 2000 the range of CCM values for the difference from 1980 for 60°S–60°N or 90°S–90°N TCO amounts is approximately 15 DU. By about 2080, the range is about 9 DU and the contribution to that range from the simulated ozone response to stratospheric chlorine change is near zero (Figure 6). The MLR analysis presented in the previous section, summarized by Figure 6, shows that understanding the differences among CCM projections requires understanding both the differences in ozone sensitivity to chlorine and the differences in ozone sensitivity to climate change, especially in the upper troposphere and lower stratosphere. To explain the narrower range for TCO return to 1980 for CCMs with most realistic transport, we demonstrate the relationship between transport and lower stratosphere distributions of chlorine reservoirs, linking those distributions with the simulated sensitivity of lower stratospheric ozone to chlorine change.

All CCMs solve a continuity equation for the ozone mixing ratio γ_{O3} at each grid point that includes chemical production (P), loss (L), and transport terms:

$$\frac{\partial \gamma_{O3}}{\partial t} = P - L + \text{transport}$$

Below about 50 km, ozone is very nearly equal to the sum of ozone and atomic oxygen, and photolysis of ozone producing atomic oxygen and reformation of ozone through reaction of atomic and molecular oxygen are in approximate balance. Production is mainly photolysis of molecular oxygen producing two oxygen atoms that form ozone molecules by reaction of atomic and molecular oxygen. In addition to the reaction of atomic oxygen with ozone, catalytic cycles involving hydrogen, nitrogen, and chlorine radicals contribute to ozone loss [e.g., *Holloway and Wayne*, 2010].

As atmospheric composition changes, realistic computation of the $\partial\gamma_{O3}/\partial t$ requires appropriate contributions from the photochemical and transport terms. A realistic estimate of the fractional change in L requires realistic representation of the fractional importance of each catalytic cycle to the total loss in an unperturbed atmosphere. Short-lived radicals (e.g., chlorine monoxide (ClO), hydroxyl (OH), and nitrogen dioxide (NO_2)) participate in catalytic ozone loss. Although radicals are short lived, transport processes affect ozone loss

©2014. American Geophysical Union. All Rights Reserved.

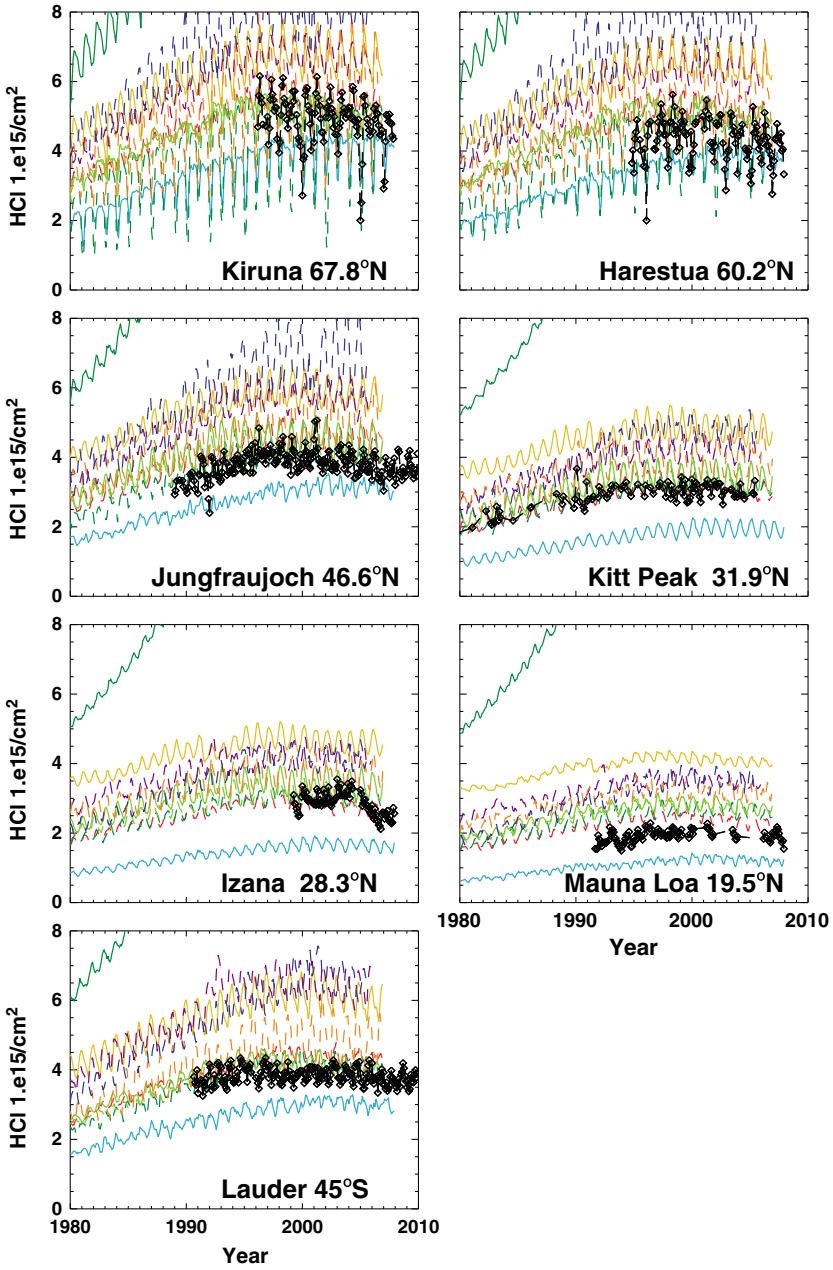

Figure 7. (a) Time series of monthly mean HCl columns (black) at seven NDACC stations spanning a latitude range 67.8°N–45°S are compared with time series obtained from CCMs (colored traces), excluding those identified as having most realistic transport. (b) Same as Figure 7a comparing time series of measurements with results from the four CCMs identified as having most realistic transport.

through their influence on the distributions of long-lived gases and reservoir gases. Source gases such as chlorofluorocarbons and N_2O produce radicals when destroyed in the stratosphere, reservoir gases such as hydrogen chloride (HCl) and chlorine nitrate ($ClONO_2$) are produced by reactions of radicals with source gases or with each other. *Dessler et al*. [1995] showed that the partitioning between $ClONO_2$ and HCl as observed by instruments on the Upper Atmosphere Research Satellite (UARS) follows expectation; the ratio $ClONO_2$/HCl is quadratically dependent on ozone, linearly dependent on the hydroxyl radical (OH), and inversely dependent on methane. In the lower stratosphere the distributions of both ozone and methane are strongly influenced by transport. Aircraft observations show little variation in OH for a given altitude and

©2014. American Geophysical Union. All Rights Reserved.

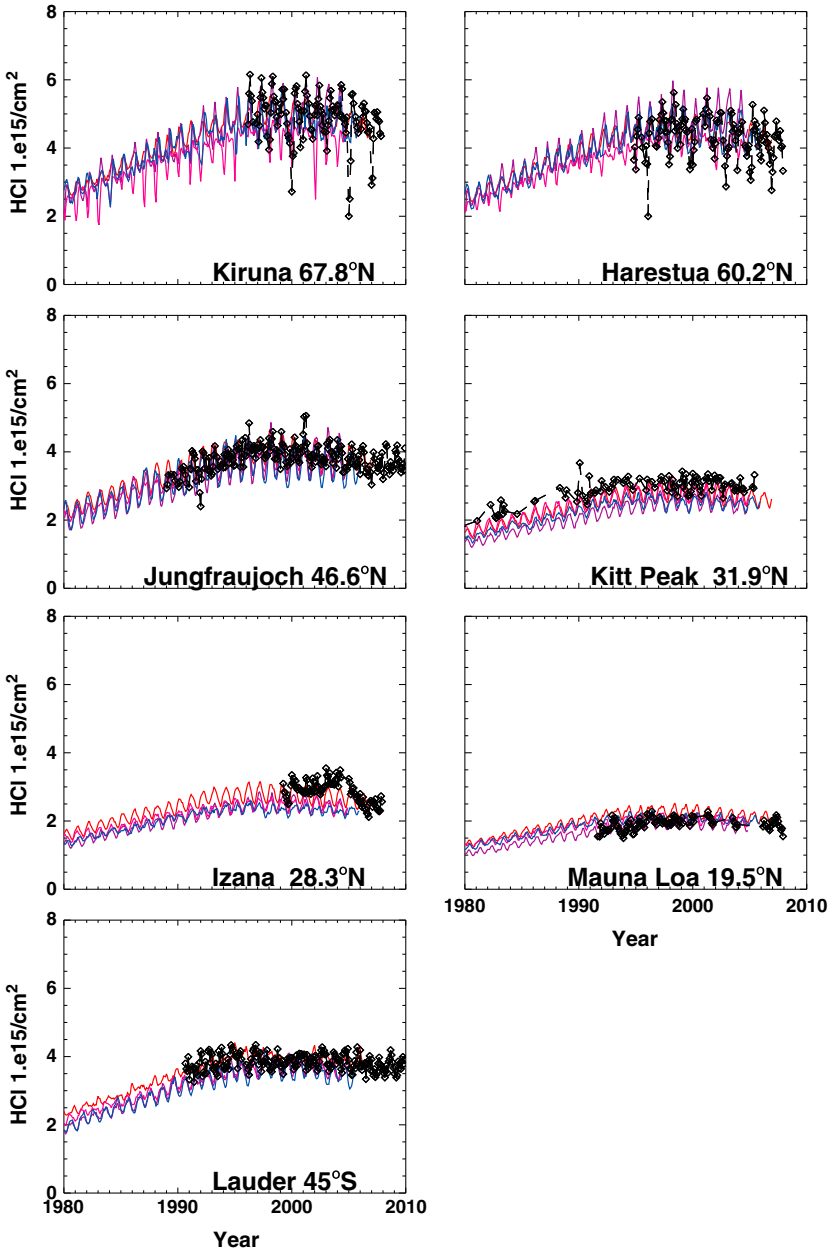

Figure 7. (continued)

fixed solar zenith angle [*Wennberg et al.*, 1994]. *Dessler et al.* [1996] showed the broad agreement between observed and expected partitioning of the reservoir $ClONO_2$ and the radical chlorine monoxide using UARS observations of ClO, NO_2, and $ClONO_2$ along with laboratory data. Thus, transport impacts the sensitivity of a CCM to chlorine change because it causes higher or lower levels of $ClONO_2$ which in turn lead to higher or lower levels of ClO in the lower stratosphere. Simulations with higher levels of ClO will have greater contributions of chlorine-catalyzed loss to the ozone tendency.

Chapter 6 of CCMVal2010 compared time series of HCl and $ClONO_2$ at the Jungfraujoch station (46.6°N) with time series simulated by CCMs; these are likely indicators of the simulated lower stratosphere sensitivity to chlorine because for both species more than 70% of the total column resides below 20 hPa. The simulated HCl columns shown in Figure 7 span a wide range of values, with peak annual mean values between 3.1×10^{15} and 6.4×10^{15} molecules/cm^2 (disregarding one CCM with an

©2014. American Geophysical Union. All Rights Reserved.

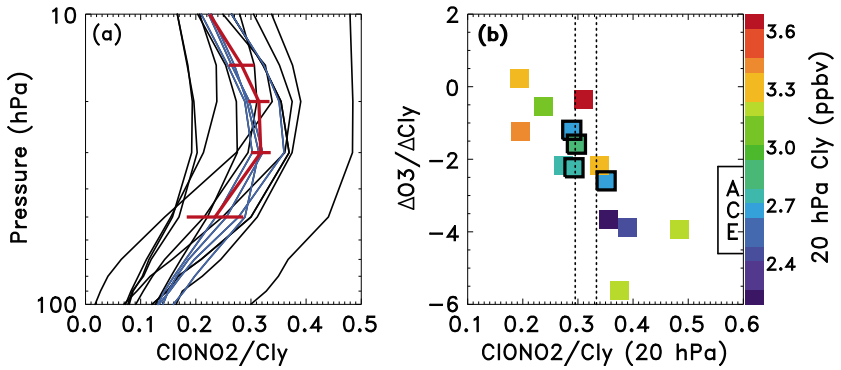

Figure 8. (a) The December 2004 mean $ClONO_2/Cl_y$ for 45°N from the ACE measurements (red solid line), from the four CCMs with most realistic transport (blue solid lines), and from the rest of the CCMs (black solid lines). Horizontal bars on the ACE profile indicate the standard deviation. (b) The sensitivity of lower atmosphere ozone to chlorine change ($\Delta O_3/\Delta Cl_y$) obtained from the MLR as a function of the simulated ratio $ClONO_2/Cl_y$ at 20 hPa. The CCMs with most realistic transport are outlined by black squares. Vertical dashed lines indicate the ACE estimate for $ClONO_2/Cl_y$ at 20 hPa. The colors of the symbols correspond to the total Cl_y at 20 hPa—the ACE estimate is indicated on the color bar. The correlation coefficient between $ClONO_2$/Cly and $\Delta O_3/\Delta Cl_y$ is −0.78.

extremely high peak value due to lack of tropospheric rainout of HCl) compared with 4.0×10^{15}, the 1998–2001 average of HCl column measurements at Jungfraujoch. The simulated columns generally exhibit the observed time dependence because the time dependence of the chlorine-containing source gases (e.g., $CFCl_3$ and CF_2Cl_2) is controlled by the boundary conditions. As discussed by *Waugh et al.* [2007, and references therein], destruction of ODSs and production of Cl_y depends on both time in the stratosphere and transport pathway. The *Strahan et al.* [2011] analysis reveals large differences in transport, consistent with large differences in lower startospheric Cl_y. Partitioning between chlorine reservoirs HCl and $ClONO_2$ depends on transported species such as CH_4. Differences in both Cl_y and its partitioning between the chlorine reservoirs contribute to the large spread in computed values of the HCl columns.

The link between transport and gas phase photochemistry in the lower stratosphere is demonstrated by comparisons of observed and simulated HCl columns in Figure 7. We use seven stations that span 68°N–45°S (Table 2) but are outside the polar vortices, avoiding large seasonal variations in their columns [*Santee et al.*, 2008]. The Figure 7a compares the monthly averages computed from observed HCl columns with CCMs, excluding those with realistic transport identified by *Strahan et al.* [2011]; Figure 7b compares the observations with time series from the remaining CCMs. For the entire latitude range, observed and simulated HCl columns are in much better agreement for simulations that perform well on transport diagnostics. Note that CCM monthly zonal means are compared with monthly means computed from observations obtained at irregular intervals throughout the year from each station; thus, observed variability appears larger.

We further investigate the partitioning between HCl and $ClONO_2$ reservoirs using observations from the ACE-FTS. Figure 8a shows profiles from the 14 CCMs of $ClONO_2/Cl_y$ between 100 hPa and 10 hPa for December 2005. This ratio is approximated by $ClONO_2/(ClONO_2 + HCl)$ for 20 hPa and higher pressures in winter. Blue lines indicate the four CCMs with most realistic transport and black lines are the others. The red line indicates the December mean of ACE-FTS profiles between 40°N and 50°N, 50 hPa–20 hPa; horizontal lines are the standard deviation of the observed profiles. The CCM with the highest values for $ClONO_2/Cl_y$ has a known error in the photochemical mechanism that leads to lower HCl. Similar comparisons are obtained for other months, and interannual variability for a single CCM for Cl_y near its maximum value is smaller than intermodel differences. Lower stratospheric Cl_y is changing slowly for the first few years of ACE operations, and the interannual variability in ACE measurements is well represented by the standard deviation for profiles in a single month.

Figure 5 shows that the contribution of chlorine processes to lower atmospheric ozone column change between 2000 and 1980 varies substantially among CCMs. Much of the variation in response is explained by

©2014. American Geophysical Union. All Rights Reserved.

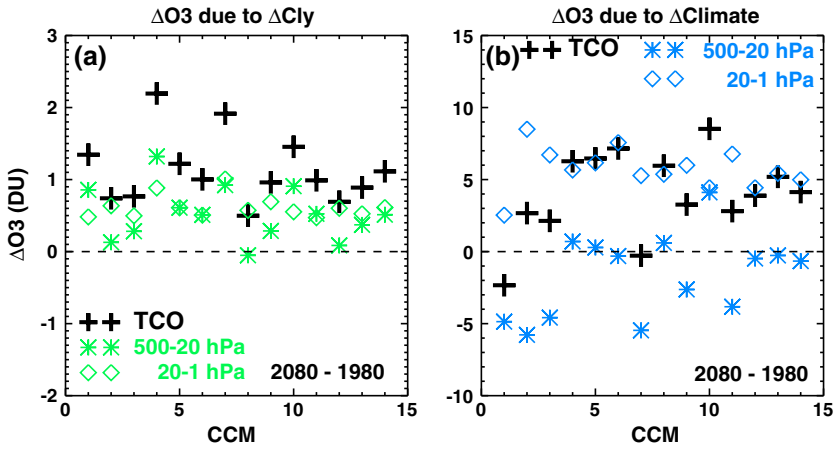

Figure 9. (a) Ozone change due to chlorine change, 2080–1980, upper stratosphere, and lower atmosphere. (b) Ozone change due to climate change, 2080–1980, upper stratosphere, and lower atmosphere.

the partitioning of chlorine reservoirs shown in Figure 8b. The sensitivity of lower stratospheric ozone to chlorine change ($\Delta O_3/\Delta Cl_y$) obtained from the MLR is shown as a function of the simulated partitioning of the chlorine reservoirs ($ClONO_2/Cl_y \approx ClONO_2/(ClONO_2 + HCl)$) at 45°N for December 2005 in Figure 8b. The symbol color indicates the total chlorine level at 20 hPa, and the range of values from ACE-FTS for December 2005, 40°N–50°N is shown on the color bar. The three CCMs that are least sensitive to chlorine change have lower than observed values of $ClONO_2/Cl_y$ and also higher than observed values for total Cl_y. The simulations that are most sensitive to chlorine have higher than observed levels of $ClONO_2/Cl_y$. The sensitivity $\Delta O_3/\Delta Cl_y$ is negatively correlated with $ClONO_2/Cl_y$ between 50 and 10 hPa for all months; similar correlations are obtained applying the MLR to middle-latitude lower stratospheric columns (35°S–60°S and 35°N–60°N), although the values of $\Delta O_3/\Delta Cl_y$ are somewhat larger (not shown). The correlation reaches its maximum value between 30 and 20 hPa (the peak for $ClONO_2/Cl_y$) during winter months and is −0.78 at 20 hPa in December. Note that observations and simulations confirm that for this pressure range distributions of reservoirs control the radical distributions [*Dessler et al.*, 1996]. *Stolarski and Douglass* [1986] and *Douglass and Stolarski* [1987] used a Monte Carlo approach in a one-dimensional model to propagate uncertainty due to reaction rates and photodissociation rates in projected stratospheric ozone response to ODS perturbations. Analysis showed larger (smaller) ozone sensitivity to chlorine change for higher (lower) levels of chlorine radicals in the "present" simulated lower stratosphere because present partitioning of chlorine species was correlated with future partitioning. The CCMs investigated here produce the same result. Simulations with higher levels of chlorine radicals inferred by partitioning of reservoirs are more sensitive to chlorine change and vice versa. The CCMs with most realistic transport have similar Cl_y levels in the lower stratosphere and similar partitioning of reservoirs, implying similar contributions of chlorine-catalyzed loss processes to ozone loss. The Cl_y levels and partitioning of reservoirs for the CCMs with most realistic transport also agree with the NDACC HCl columns and the observations from ACE-FTS. This result and the similar TCO increases due to climate change for the CCMs with most realistic transport (shown in Figure 4) explain narrower range for year of return to 1980 for CCMs with realistic performance on transport diagnostics discussed by *Strahan et al.* [2011].

As chlorine decreases, the chlorine contribution to the total change in ozone decreases and differences in chlorine reservoir distributions caused by differences in lower stratospheric transport contribute less to the variance in simulated ozone. Figure 6 shows that after 2035 the differences in the response to climate change make the larger contribution to the spread among the CCM projections.

5. Stratospheric Ozone After 2035

The contributions to ozone change for 1980–2080 from chlorine change and from climate change are compared in Figure 9. Although the anthropogenic contribution to Cl_y is not zero, the Cl_y level in 2080 is less

©2014. American Geophysical Union. All Rights Reserved.

than the 1980 level, and the annually averaged 60°S to 60°N total column ozone change relative to 1980 due to chlorine change is always positive, falling between 0.5 and 2.2 DU (Figure 9a). The ozone change due to chlorine change is always positive in the upper stratosphere and is positive in the lower stratosphere with one exception because for all but one CCM the anthropogenic contribution to stratospheric chlorine is smaller in 2080 than in 1980. Chlorine plays a small role compared with climate change, as shown in Figure 9b (note different scales for the *y* axis).

Climate change affects ozone through cooling and through changes in circulation. All CCMs predict a speedup in the Brewer-Dobson circulation, leading to ozone decreases in the tropical lower stratosphere and increases at middle and high latitudes. Stratospheric cooling results in slower rates of ozone loss processes, producing increased ozone. Twelve of the CCMs produce a net ozone increase relative to their 1980 level by 2060 as impact of chlorine change decreases. The largest predicted increase for 2080 relative to 1980 due to processes related to climate change is greater than 8 DU.

The changes in TCO and the separate contributions from the upper stratosphere (20 hPa–1 hPa partial O_3 column) and lower region (500 hPa–20 hPa partial O_3 column) due to climate-related processes are shown in Figure 9b. The standard deviation of the total column ozone increase due to climate change (~3 DU) is comparable to the multimodel mean increase (~4 DU). This large variance is caused by a bimodal distribution in model differences between the upper and lower partial O_3 columns. In the upper stratosphere, the CCMs consistently produce an ozone increase. In the lower region, seven of the CCMs predict a contribution of ±1 DU for the 60°S–60°N area-weighted mean O_3. For these CCMs the TCO response to climate change is controlled by the upper stratosphere. The mean TCO increase for these seven CCMs is about 5.6 DU, with a standard deviation of 1.2 DU. This result is consistent with analysis of GEOSCCM reported by *Li et al*. [2009], showing near cancelation of tropical and extratropical ozone changes in the upper troposphere and lower stratosphere that lead to a small net value for the area-weighted global mean change. *Li et al*. [2009] show that the TCO increase due to climate change is approximately equal to the increase in the upper stratosphere in GEOSCCM. In six of the remaining CCMs, the ozone decrease in the lower tropical stratosphere due to increased tropical upwelling exceeds extratropical increases such that the latitudinally averaged response to climate change is negative. In these six CCMs the decrease in the area-weighted 60°S–60°N mean lower stratospheric ozone is opposed by the upper stratosphere increase; mean TCO response is smaller (2.3 DU), but the standard deviation is larger (3.6 DU) compared with the seven CCMs with small contributions from lower stratosphere. In one CCM the extratropical increase exceeds the tropical decrease; the increases in the area-weighted 60°S–60°N mean in both upper and lower stratosphere combine to produce the TCO increase of more than 8 DU.

Although complete information is not available for these 14 CCMs, this difference in the net lower stratospheric ozone response appears to be linked to differences in the simulated increases in upwelling. For example, Figure 4.11 in CCMVal2010 shows that the nine CCMs producing time series longer than 100 years fall into two groups. The annual mean upward mass flux at 70 hPa as calculated from w^* for a "high" group containing five CCMs shows increases from a 1960 value ~5.8×10^9 kg/s to values as high as 7–9.2×10^9 kg/s. In contrast, the annual mean upward mass flux at 70 hPa for a "low" group containing four CCMs is initially ~4.8×10^9 kg/s and increases to 6–6.5×10^9 kg/s. The simulations considered here that are also included in CCMVal2010 Figure 4.11 separate into two groups based largely on this change in mass flux. The CCMs in the high group all produce substantial net decreases due to climate change in the 60°S–60°N 500 hPa–20 hPa partial ozone column; the CCMs in the low group all produce small net changes, with extratropical partial column ozone increases compensating for tropical partial column ozone decreases.

Although changes in the upper partial ozone column (20 hPa–1 hPa) and lower partial ozone column (500 hPa–20 hPa) both contribute to the range of CCM responses, the range of responses in the upper region is smaller than that of the lower region. *Douglass et al*. [2012] considered the response of upper stratospheric ozone in detail, showing that differences in responses to temperature change are partially explained by the simulated ozone levels themselves. CCMs that produce higher (lower) ozone levels for the 1960–1980 time frame are more (less) sensitive to temperature change because the most temperature-dependent loss process $O + O_3$ contributes more (less) to the net ozone loss. Although this is not the only factor that affects the simulated response, this approach does give insight into the responses of the outliers. The CCM that produces the largest ozone response to climate change ($>$ 8 DU) in the upper region also produces the largest unperturbed ozone

©2014. American Geophysical Union. All Rights Reserved.

partial column for 20 hPa–1 hPa, exceeding the multimodel mean by more than 15%. In contrast, the CCM that produces the smallest ozone response to climate change (< 3 DU) in the upper region produces an unperturbed partial ozone column for 20 hPa–1 hPa that is about 15% less than the multimodel mean.

To summarize, compensation or lack thereof between the decrease in tropical lower stratospheric ozone and middle- and high-latitude increases in the upper troposphere and lower stratosphere contributes much to the range of simulated responses, but whether or not such compensation is produced is not related to performance on the transport diagnostics used in Chapter 6 of CCMVal2010 or by *Strahan et al*. [2011]. Figure 1 shows that the CCMs identified with best performance on transport diagnostics separate after about 2050, with projections of ozone increases for 2 CCMs each at the high and low ends of the range for the 14 CCMs. For the CCMs included in Figure 4.11 of CCMVal2010, the CCMs that project smaller changes in the 60°S–60 N total column ozone fall in the group with high change in mass flux (larger net decrease in the lower stratosphere and upper troposphere opposing an upper stratospheric ozone increase resulting in smaller 60°S–60°N mean TCO increase). Conversely, CCMs that project large changes in the 60°S–60 N total column ozone produce smaller changes in mass flux (near cancelation between the ozone decrease in the tropical lower stratosphere and extratropical increase in the lower stratosphere and upper troposphere), resulting in larger 60°S–60°N mean TCO increases that are dominated by ozone increase in the upper stratosphere.

The response of the circulation to climate change is robust among the CCMs in the sense that all CCMs predict an increase of tropical upwelling; however, other aspects of the circulation response differ. First, the rate of increase varies, and in some of the CCMs the appearance and disappearance of the ozone hole affects the rate of increase. For example, *Oman et al*. [2009] show that in the GEOSCCM the rate of increase is faster during the formation phase of the ozone hole and slower as the ozone hole dissipates compared with the rate of increase in 2080 and beyond when ODS change ceases to be significant. Note that GEOSCCM is in the group with low change in annual mean upward mass flux at 70 hPa. Analysis of the time dependence of the annual mean upwelling for the subset of CCMs that provide time series of w^* shows that the rate of increase may be faster, slower, or unaffected by ozone hole formation and dissipation. *Lin and Fu* [2013] investigate acceleration of the Brewer-Dobson circulation in the same group of CCMs in more detail, dividing the Brewer-Dobson circulation into branches based on hemispheric location and vertical extent. Although in most CCMs the increase in the Brewer-Dobson circulation due to GHG increase is reinforced by ozone depletion and opposed by ozone recovery in its deep branch (above 30 hPa) in the Southern Hemisphere during austral summer, an ozone effect on the Brewer-Dobson circulation is less evident during other seasons or in the lower branches. Second, the extratropical circulation changes and their convolution with simulated lower stratospheric ozone vary substantially. There are differences in both the tropical lower stratosphere ozone decrease and in the extratropical ozone increase in the upper troposphere and lower stratosphere that result in near cancelation or lack thereof. Both of these factors contribute to the differences among CCM projections for 21st century ozone.

6. Conclusions

This work quantifies the ozone response to changes in chlorine-containing source gases and changing climate (i.e., stratospheric cooling and circulation change) in 14 CCMs that participated in CCMVal and contributed simulations to WMO2010. All models used the same time-dependent mixing ratio boundary conditions for source gases from 1960 to 2100. In 2035, the chlorine contribution to ozone change relative to 1980 is negative in all CCMs, not surprising since chlorine is still substantially elevated compared with 1980; the climate change contribution for 1980–2035 is positive in most but not all CCMs. The 60°S–60°N annual mean ozone is within 2 DU of 1980 levels (i.e., ΔTCO < 1%) for 10 of the CCMs by 2035.

Strahan et al. [2011] showed a narrower range of recovery dates for the CCMs with best performance on the CCMVal transport diagnostics compared with the range for the entire group. This work shows that differences in ozone sensitivity to chlorine change contribute more to the spread in years for return to 1980 than differences in ozone sensitivity to climate change. These differences in chlorine sensitivity are explained by differences in the middle-latitude lower stratospheric columns of chlorine reservoirs and differences in partitioning between HCl and $ClONO_2$. The transport diagnostics narrow the range of responses because they select CCMs with a much narrower and more realistic range of column values and partitioning among chlorine reservoirs than produced by the suite of CCMs. By 2035 12 of 14 CCMs show an ozone increase in 60°S–60°N TCO due to climate change that is between 1 and 4 DU. The CCMs with latest recovery are either

©2014. American Geophysical Union. All Rights Reserved.

more sensitive to chlorine change or less sensitive to climate change than the CCMs identified as having most realistic transport. The CCM with much earlier recovery is least sensitive to chlorine change and among the most sensitive to climate change.

We emphasize the value of the comparisons with NDACC column measurements of the chlorine reservoirs along with comparisons of partitioning among chlorine reservoirs obtained from ACE $ClONO_2$ and HCl profiles, as these comparisons provide a mechanism to explain the variation in the sensitivity to chlorine change by linking lower stratospheric transport with chemistry through the control of the distributions of chlorine reservoir species. CCMs that are most sensitive to chlorine have higher values for $ClONO_2/Cl_y$. The column amounts of HCl and $ClONO_2$ depend both on total Cl_y in the lower atmosphere and its partitioning between the chlorine reservoirs. Because of the mixing ratio boundary conditions, stratospheric Cl_y can vary widely depending on the simulated transport. However, the CCMs with the highest levels of lower stratospheric Cl_y need not be the most sensitive to chlorine change, if they partition chlorine reservoirs toward HCl at the expense of $ClONO_2$. The ozone response to chlorine change depends on reactions with short-lived radical species whose levels are controlled by both the total Cl_y and its partitioning between the reservoir species HCl and $ClONO_2$.

In 2035, the simulated response of ozone to climate change is between 1.3 and 4 DU for the CCMs with most realistic transport; for 12 of the 14 CCMs the response to climate change is positive and between 1 and 4.5 DU. As the simulations continue, differences in the ozone response to changes in circulation and temperature grow. In the upper stratosphere the 60°S–60°N annual average ozone increases in all CCMs, and the differences in the magnitude of the increase are explained by differences in the importance of the various catalytic loss cycles, such that simulations with highest ozone in the unperturbed (low chlorine) period (~1960– ~ 1980) are most sensitive to temperature change [*Douglass et al.*, 2012]. These differences account for about one third of the spread in projections. The ozone response in the lower stratosphere and upper troposphere is more complicated, as both circulation change and temperature change contribute. Although the CCMs all predict increased upwelling, the rate of increase varies among CCMs. *Oman et al.* [2009] show a much larger rate of increase in w^* during ozone hole formation than during ozone hole dissipation for GEOSCCM. There is no consensus among CCMs as to the impact of the ozone hole on the rate of increase of w^*. *Li et al.* [2009] note that the speedup of the Brewer-Dobson circulation produces a decrease in the tropical lower stratospheric ozone that is nearly canceled by middle- and high-latitude ozone increases in the lower stratosphere and upper troposphere when a broad latitudinal average is considered. Seven of the fourteen CCMs (including GEOSCCM) behave in a similar manner, and the 60°S–60°N mean ozone change due to climate change for this subgroup is positive and less than 1 DU for 2080 relative to 1980. For six of the remaining CCMs ozone change due to upwelling in the tropical lower stratosphere exceeds the extratropical increases, resulting in a net negative contribution from the lower stratosphere (-4.5 ± 1 DU). For one CCM the net contribution from the lower stratosphere due to climate change is substantially positive. These differences contribute most to the differences in projections in the late 21st century. The CCMVal transport diagnostics do not discriminate among the projections for w^* or the cancelation between tropical and extratropical responses. Reduction of the spread among projections for future ozone levels requires further investigation in the differences in the response of the Brewer-Dobson circulation to increasing GHGs.

This analysis shows that most differences among projections for ozone can be explained. *Douglass et al.* [2012] show that differences in the temperature and trace gases such as nitrogen oxides lead to differences in the relative importance of loss processes that control the upper stratospheric ozone level, explaining differences in the upper stratospheric ozone responses to changes in chlorine and temperature. Observations are therefore fundamental to identifying CCMs with appropriate contributions from each loss process in order to identify the "best" projection. Similarly, the near-linear dependence of the ozone sensitivity to chlorine on the partitioning between $ClONO_2$ and HCl suggests that lower stratospheric ozone responses to chlorine change will be similar if the reservoir distributions are similar. Therefore, it is important to use observations such as NDACC columns and profiles from ACE-FTS to assure that the reservoir distributions are realistic. In this case, deficiencies in transport relate directly to differences in the simulated response of ozone to composition change. The lower stratospheric ozone evolution is simple to diagnose given the evolution of w^*. Although it is not possible at this time to explain differences among simulations for w^*, it is likely that as data records lengthen, analysis of observations in the tropics will provide limits for the rate of change of w^* using such

©2014. American Geophysical Union. All Rights Reserved.

quantities as the lower stratospheric ozone or the amplitude of the quasi-biennial oscillation [*Randel and Thompson*, 2011; *Kawatani and Hamilton*, 2013].

Finally, these results, in particular linking transport diagnostics, unrealistic reservoir distributions, and differences in sensitivity of simulated lower atmospheric ozone to chlorine change, question the value of the use of a multimodel mean as a best projection of 21st century ozone. Differences in simulated responses that can be traced to biases that are understood and clearly not random. This study has identified causes for differences in CCM ozone projections and explained the differences in lower stratosphere sensitivity to chlorine change. This work demonstrates that diagnostics used to evaluate CCM performance are most useful when they are linked with a mechanism that is related to a model's response to a perturbation. The use of such diagnostics supports a strategy to reduce uncertainty in projections.

Acknowledgments

We acknowledge the modeling groups for making their simulations available for this analysis. The Chemistry-Climate Model Validation Activity (CCMVal) for WCRP's (World Climate Research Programme) SPARC (Stratosphere-troposphere Processes and their Role in Climate) project for organizing and coordinating the model data analysis activity and the British Atmospheric Data Center (BADC) for collecting and archiving the CCMVal model output. The data used in this publication were obtained as part of the Network for the Detection of Atmospheric Composition Change (NDACC) and are publicly available (see http://www.ndacc.org). We appreciate helpful comments from three anonymous reviewers. This work is supported by NASA's Atmospheric Chemistry Modeling and Analysis Program (ACMAP) and Modeling and Analysis Program (MAP).

References

Akiyoshi, H., L. B. Zhou, Y. Yamashita, K. Sakamoto, M. Yoshiki, T. Nagashima, M. Takahashi, J. Kurokawa, M. Takigawa, and T. Imamura (2009), A CCM simulation of the breakup of the Antarctic polar vortex in the years 1980–2004 under the CCMVal scenarios, *J. Geophys. Res.*, *114*, D03103, doi:10.1029/2007JD009261.

Austin, J., and R. J. Wilson (2006), Ensemble simulations of the decline and recovery of stratospheric ozone, *J. Geophys. Res.*, *111*, D16314, doi:10.1029/2005JD006907.

Austin, J., and R. J. Wilson (2010), Sensitivity of polar ozone to sea surface temperatures and halogen amounts, *J. Geophys. Res.*, *115*, D18303, doi:10.1029/2009JD013292.

Bekki, S. and G. E. Bodeker (Coordinating Lead Authors) et al. (2011), Future ozone and its impact on surface UV, Chapter 3 in *Scientific Assessment of Ozone Depletion*: *2010*, Global Ozone Research and Monitoring Project—Report No. 52, 516 pp., World Meteorological Organization, Geneva, Switz.

Bernath, P. F., et al. (2005), Atmospheric Chemistry Experiment (ACE): Mission overview, *Geophys. Res. Lett.*, *32*, L15S01, doi:10.1029/2005GL022386.

Butchart, N., et al. (2006), Simulations of anthropogenic change in the strength of the Brewer-Dobson circulation, *Clim. Dyn.*, *27*, 727–741.

Butchart, N., et al. (2010), Chemistry–climate model simulations of twenty-first century stratospheric climate and circulation changes, *J. Clim.*, *23*, 5349–5373.

Davies, T., M. J. P. Cullen, A. J. Malcolm, M. H. Mawson, A. Staniforth, A. A. White, and N. Wood (2005), A new dynamical core for the Met Office's global and regional modelling of the atmosphere, *Q. J. R. Meteorol. Soc.*, *131*, 1759–1782, doi:10.1256/qj.04.101.

de Grandpré, J., S. R. Beagley, V. I. Fomichev, E. Griffioen, J. C. McConnell, A. S. Medvedev, and T. G. Shepherd (2000), Ozone climatology using interactive chemistry: Results from the Canadian Middle Atmosphere Model, *J. Geophys. Res.*, *105*, 26,475–26,491, doi:10.1029/2000JD900427.

Dessler, A. E., et al. (1995), Correlated observations of HCl and $ClONO_2$ from UARS and implications for stratospheric chlorine partitioning, *Geophys. Res. Lett.*, *22*, 1721–1724.

Dessler, A. E., R. Kawa, A. Douglass, D. Considine, J. Kumer, J. Waters, and J. Gille (1996), A test of the partitioning between ClO and $ClONO_2$ based on simultaneous UARS measurements of ClO, NO_2, and $ClONO_2$, *J. Geophys. Res.*, *101*, 12,515–12,521.

Déqué, M. (2007), Frequency of precipitation and temperature extremes over France in an anthropogenic scenario: Model results and statistical correction according to observed values, *Global Planet. Change*, *57*, 16–26, doi:10.1016/j.gloplacha.2006.11.030.

Douglass, A. R., and R. S. Stolarski (1987), The use of atmospheric measurements to constrain model predictions of ozone change from chlorine perturbations, *J. Geophys. Res.*, *92*, 6662–6674.

Douglass, A. R. and V. Fioletov (Coordinating Lead Authors), S. Godin-Beekman, R. Müller, R. S. Stolarski, and A. Webb (2011), Stratospheric ozone and surface ultraviolet radiation, chapter 2 in *Scientific Assessment of Ozone Depletion: 2010*, Global Ozone Research and Monitoring Project Report No. 52, World Meteorological Organization, Geneva, Switz.

Douglass, A. R., R. S. Stolarski, S. E. Strahan, and L. D. Oman (2012), Understanding differences in upper stratospheric ozone response to changes in chlorine and temperature as computed using CCMVal-2 models, *J. Geophys. Res.*, *117*, D16306, doi:10.1029/2012JD017483.

Eyring, V., et al. (2005), A strategy for process-oriented validation of coupled chemistry-climate models, *Bull. Am. Meteorol. Soc.*, *86*, 1117–1133.

Garcia, R. R., D. Marsh, D. E. Kinnison, B. Boville, and F. Sassi (2007), Simulations of secular trends in the middle atmosphere, 1950–2003, *J. Geophys. Res.*, *112*, D09301, doi:10.1029/2006JD007485.

Haigh, J. D., and J. A. Pyle (1982), Ozone perturbation experiments in a two-dimensional circulation model, *Quart. J. R. Met. Socl.*, *108*, 5510–574, doi:10.1002/qj.49710845705.

Holloway, A. M., and R. P. Wayne (2010), *Atmospheric Chemistry*, The Royal Society of Chemistry, Cambridge, U. K.

IPCC (Intergovernmental Panel on Climate Change) (2000), *Special Report on Emissions Scenarios*: *A Special Report of Working Group III of the Intergovernmental Panel on Climate Change*, 599 pp., Cambridge Univ. Press, Cambridge, U. K.

Jourdain, L., S. Bekki, F. Lott, and F. Lefevre (2008), The coupled chemistry-climate model LMDZ-REPROBUS: Description and evaluation of a transient simulation of the period 1980–1999, *Ann. Geophys.*, *26*, 1391–1413, doi:10.5194/angeo-26-1391-2008.

Kawatani, Y., and K. Hamilton (2013), Weakened stratospheric quasibiennial oscillation driven by increased tropical mean upwelling, *Nature*, *497*, 478–482, doi:10.1038/nature12140.

Kohlhepp, R., et al. (2012), Observed and simulated time evolution of HCl, $ClONO_2$, and HF total column abundances, *Atmos. Chem. Phys.*, *12*, 3527–3557, doi:10.5194/acp-12-3527-2012.

Li, F., R. S. Stolarski, and P. A. Newman (2009), Stratospheric ozone in the post-CFC era, *Atmos. Chem. Phys.*, *9*, 2207–2213, doi:10.5194/acp-9-2207-2009.

Lin, P., and Q. Fu (2013), Changes in various branches of the Brewer-Dobson circulation from an ensemble of chemistry climate models, *J. Geophys. Res. Atmos.*, *118*, 73–84, doi:10.1029/2012JD018813.

Mahieu, E., et al. (2005), Comparisons between ACE-FTS and ground-based measurements of stratospheric HCl and $ClONO_2$ loadings at northern latitudes, *Geophys. Res. Lett.*, *32*, L15S08, doi:10.1029/2005GL022396.

©2014. American Geophysical Union. All Rights Reserved.

Morgenstern, O., P. Braesicke, F. M. O'Connor, A. C. Bushell, C. E. Johnson, S. M. Osprey, and J. A. Pyle (2009), Evaluation of the new UKCA climate composition model. Part 1: The stratosphere, *Geosci. Model Dev.*, *2*, 43–57, doi:10.5194/gmd-2-43-2009.

Morgenstern, O., et al. (2010), Review of the formulation of present generation stratospheric chemistry-climate models and associated external forcings, *J. Geophys. Res.*, *115*, D00M02, doi:10.1029/2009JD013728.

Newman, P. A., J. Daniel, D. Waugh, and E. Nash (2007), A new formulation of equivalent effective stratospheric chlorine (EESC), *Atmos. Chem. Phys.*, *7*, 4537–4552.

Oman, L. D., D. W. Waugh, S. Pawson, R. S. Stolarski, and P. A. Newman (2009), On the influence of anthropogenic forcings on changes in the stratospheric mean age, *J. Geophys. Res.*, *114*, D03105, doi:10.1029/2008JD010378.

Oman, L. D., et al. (2010), Multimodel assessment of the factors driving stratospheric ozone evolution over the 21st century, *J. Geophys. Res.*, *115*, D24306, doi:10.1029/2010JD014362.

Pawson, S., R. S. Stolarski, A. R. Douglass, P. A. Newman, J. E. Nielsen, S. M. Frith, and M. L. Gupta (2008), Goddard Earth Observing System chemistry-climate model simulations of stratospheric ozone-temperature between 1950 and 2005, *J. Geophys. Res.*, *113*, D12103, doi:10.1029/2007JD009511.

Pitari, G., E. Mancini, V. Rizi, and D. T. Shindell (2002), Impact of future climate and emission changes on stratospheric aerosols and ozone, *J. Atmos. Sci.*, *59*, 414–440, doi:10.1175/1520-0469.

Randel, W. J., and A. M. Thompson (2011), Interannual variability and trends in tropical ozone derived from SAGE II satellite data and SHADOZ ozonesondes, *J. Geophys. Res.*, *116*, D07303, doi:10.1029/2010JD015195.

Rinsland, C. P., et al. (2003), Long-term trends of inorganic chlorine from ground-based infrared solar spectra: Past increases and evidence for stabilization, *J. Geophys. Res.*, *108*(D8), 4252, doi:10.1029/2002JD003001.

Santee, M. L., I. A. MacKenzie, G. L. Manney, M. P. Chipperfield, P. F. Bernath, K. A. Walker, C. D. Boone, L. Froidevaux, N. J. Livesey, and J. W. Waters (2008), A study of stratospheric chlorine partitioning based on new satellite measurements and modeling, *J. Geophys. Res.*, *113*, D12307, doi:10.1029/2007JD009057.

Schraner, M., et al. (2008), Technical note: Chemistry-climate model SOCOL: Version 2.0 with improved transport and chemistry/microphysics schemes, *Atmos. Chem. Phys.*, *8*, 5957–5974, doi:10.5194/acp-8-5957-2008.

Scinocca, J. F., N. A. McFarlane, M. Lazare, J. Li, and D. Plummer (2008), Technical note: The CCCma third generation AGCM and its extension into the middle atmosphere, *Atmos. Chem. Phys.*, *8*, 7055–7074, doi:10.5194/acp-8-7055-2008.

Scinocca, J. F., D. B. Stephenson, T. C. Bailey, and J. Austin (2010), Estimates of past and future ozone trends from multi-model simulations using a flexible smoothing spline methodology, *J. Geophys. Res.*, *115*, D00M12, doi:10.1029/2009/JD013622.

Shepherd, T. G. (2008), Dynamics, stratospheric ozone, and climate change, *Atmos. Ocean*, *46*, 117–138, doi:10.3137/ao.460106.

Shibata, K., and M. Deushi (2008a), Long-term variations and trends in the simulation of the middle atmosphere 1980–2004 by the chemistry climate model of the Meteorological Research Institute, *Ann. Geophys.*, *26*, 1299–1326, doi:10.5194/angeo-26-1299-2008.

Shibata, K., and M. Deushi (2008b), *Simulation of the Stratospheric Circulation and Ozone During the Recent Past (1980–2004) With the MRI Chemistry-Climate Model, CGER's Supercomp*, *Monogr. Rep.*, vol. 14, 154 pp., Cent. for Gobal Environ. Res., Natl. Inst. For Environ. Studies, Tsukuba, Japan.

SPARC CCMVal (2010), SPARC report on the evaluation of chemistry-climate models, edited by V. Eyring et al., SPARC Report No. 5, WcRP-32, WMO/TD-No. 1526.

Stolarski, R. S., and A. R. Douglass (1985), Parameterization of the photochemistry of stratospheric ozone including catalytic loss processes, *J. Geophys. Res.*, *90*, 10,709–10,718.

Stolarski, R. S., and A. R. Douglass (1986), Sensitivity of an atmospheric photochemistry model to chlorine perturbations including consideration of uncertainty propagation, *J. Geophys. Res.*, *91*, 7853–7864.

Stolarski, R. S., P. Bloomfield, R. D. McPeters, and J. R. Herman (1991), Total ozone trends deduced from nimbus 7 TOMS data, *Geophys. Res. Lett.*, *6*, 1015–1018.

Stolarski, R. S., A. R. Douglass, S. Steenrod, and S. Pawson (2006), Trends in stratospheric ozone: Lessons learned from a 3D chemical transport model, *J. Atmos. Sci.*, *63*, 1028–1041.

Stolarski, R. S., A. R. Douglass, P. A. Newman, S. Pawson, and M. R. Schoeberl (2010), Relative contribution of greenhouse gases and ozone-depleting substances to temperature trends in the stratosphere: A chemistry-climate model study, *J. Clim.*, *23*, 28–41.

Strahan, S. E., et al. (2011), Using transport diagnostics to understand chemistry climate model ozone simulations, *J. Geophys. Res.*, *116*, D17302, doi:10.1029/2010JD015360.

Teyssèdre, H., et al. (2007), A new tropospheric and stratospheric chemistry and transport model MOCAGE-Climate for multi-year studies: Evaluation of the present-day climatology and sensitivity to surface processes, *Atmos. Chem. Phys.*, *7*, 5815–5860, doi:10.5194/acp-7-5815-2007.

Tian, W., and M. P. Chipperfield (2005), A new coupled chemistry-climate of the stratosphere: The importance of coupling for future O3-climate predictions, *Q. J. R. Meteorol. Soc.*, *131*, 281–303, doi:10.1256/qj.04.05.

Tian, W., M. P. Chipperfield, L. J. Gray, and J. M. Zawodny (2006), Quasibiennial oscillation and tracer distributions in a coupled chemistry-climate model, *J. Geophys. Res.*, *111*, D20301, doi:10.1029/2005JD006871.

Waugh, D. W., S. E. Strahan, and P. A. Newman (2007), Sensitivity of stratospheric inorganic chlorine to differences in transport, *Atmos. Chem. Phys.*, *7*, 4935–4941.

Waugh, D. W., and V. Eyring (2008), Quantitative performance metrics for stratospheric-resolving chemistry-climate models, *Atmos. Chem. Phys.*, *8*, 5699–5713.

Waugh, D. W., L. Oman, S. R. Kawa, R. S. Stolarski, S. Pawson, A. R. Douglass, P. A. Newman, and J. E. Nielsen (2009), Impacts of climate change on stratospheric ozone recovery, *Geophys. Res. Lett.*, *36*, L03805, doi:10.1029/2008GL036223.

Wennberg, P. O., et al. (1994), Removal of stratospheric O_3 by radicals: In situ measurements of OH, HO_2, NO, NO_2, ClO and BrO, *Science*, *266*, 398–403.

WMO (World Meteorological Organization) (2007), Scientific assessment of ozone depletion: 2006, Global Ozone Research and Monitoring Project–Report No. 50, 572 pp., Geneva, Switz.

WMO (World Meteorological Organization) (2011), Scientific Assessment of Ozone Depletion: 2010: Global Ozone Research and Monitoring Project – Report No. 52, 516 pp., Geneva, Switz.

©2014. American Geophysical Union. All Rights Reserved.